Stoch Environ Res Risk Assess (2016) 30:1421–1440
DOI 10.1007/s00477-015-1149-7

ORIGINAL PAPER

Spatio-temporal characteristics of extreme precipitation events during 1951–2011 in Shandong, China and possible connection to the large scale atmospheric circulation

Tao Gao[1,3] · **Xiaohui Shi**[2]

Published online: 3 September 2015

Abstract Analyses of the spatio-temporal variability of precipitation extremes defined by eleven extreme precipitation indices in Shandong were conducted by utilizing the methods of linear regression, ensemble empirical mode decomposition (EEMD) and Mann–Kendall test. The results revealed that statistically significant decreasing trends existed for almost all extreme precipitation indices except for the consecutive dry days (CDD) and simple daily intensity index. A periodicity of 10–15 years for precipitation extremes is detected by EEMD analysis. Greatest 5-day total rainfall (RX5day), very wet days (R95p) and annual total wet-day precipitation (PRCPTOT) experienced decreasing trends in the region stretching from the southeast coast to the west, while the spatial distribution of the decreasing trends for other indices was more complicated. Moreover, the frequency of occurrence in precipitation extremes at Changdao station, surrounded by the sea in the northeast region, increased in contrast to surrounding stations. This may suggest a possible effect from the local marine environment on extreme precipitation. In addition, the stations with statistically significant positive trends for CDD were mainly located in mid-west Shandong and along the southeast coast, where the extreme precipitation and total rainfall were, on the contrary, characterized by decreasing trends. These results indicate that drought or severe drought events have become more frequent in those regions. Analysis of large-scale atmospheric circulation changes indicates that a strengthening anticyclonic circulation and increasing geopotential height as well as decreasing strength of monsoonal flow in recent decades may have contributed to the variations in extreme precipitation in Shandong.

Keywords Extreme precipitation events · Ensemble empirical mode decomposition (EEMD) · Atmospheric circulation · Shandong Province

1 Introduction

The fifth assessment report of the Intergovernmental Panel on Climate Change (IPCC AR5) pointed out that global annual mean temperature increased by 0.85 °C during 1880–2012 (IPCC 2014; Pachauri et al. 2014), which is one of the main challenges facing humanity in the 21st century. Since a warmer atmosphere could hold more moisture according to the Clausius–Clapeyron relation, global warming is inevitably associated with the recent increases of extreme precipitation events owing to the increased atmospheric water vapor and warmer atmosphere (O'Gorman and Schneider 2009; Grimm 2011; Sillmann et al. 2013; Mallakpour and Villarini 2015). In addition, it is widely recognized that the variability in the frequency and intensity of extreme climate and weather events have significant adverse impacts on society and environmental sustainability and devastating economic losses (Easterling

Electronic supplementary material The online version of this article (doi:10.1007/s00477-015-1149-7) contains supplementary material, which is available to authorized users.

✉ Xiaohui Shi
sxh@cams.cma.gov.cn

[1] Department of Resources and Environmental Sciences, Heze University, Heze 274015, China

[2] State Key Laboratory of Severe Weather, Chinese Academy of Meteorological Sciences, Beijing 100081, China

[3] Key Laboratory of Marine Environment and Ecology, Ministry of Education, Ocean University of China, Qingdao 266100, China

et al. 2000; Groisman et al. 1999; Bocheva et al. 2009; Peterson et al. 2013). As a result, increasing concerns on extreme climate events, extreme precipitation in particular, have been drawn from the public, government and meteorological communities over the world during recent decades (e.g., Alexander et al. 2006; Wuebbles et al. 2014; You et al. 2011).

Compared to extreme temperature changes, variations of precipitation extremes show more distinctive regional characteristics. Iwashima and Yamamoto (1993) studied the long-term trend of heavy daily precipitation in Japan and reported that the number of days with heavy rainfall has increased. Similar phenomena were also investigated over the United States by Karl et al. (1996), who reported that the contribution of 1-day precipitation events exceeding 50.8 mm to total annual precipitation has increased from about 9 % in the 1910s to about 11 % in the 1980s and 1990s. In the mid-latitude regions of Europe, all Europe-average indices of precipitation extremes increased during 1946–1999, although the spatial coherence of the trends is low (Klein Tank and Können 2003; Moberg et al. 2006). Meanwhile, the potential occurrences of daily precipitation exceeding 50.8 mm in mid-latitude countries including the United States, Australia, Mexico, and China increased by approximately 20 % in the late 20th century (Groisman et al. 1999). In general, the observed changes in intense precipitation, including the frequency of very heavy precipitation or the upper 0.3 % of daily precipitation events, have been analyzed for over half of the land area of the globe, and there has been a widespread increase in the frequency of very heavy precipitation in the mid-latitudes during the past 50–100 year (Groisman et al. 2005).

In China, variations in precipitation extremes have been examined extensively both at the national and regional scales. By analyzing the trend in normalized annual precipitation anomalies and in some annual extremes during 1951–1995, Zhai et al. (1999) suggested that changes in extreme and total precipitation might be closely related to each other and northwest China was the region that might have experienced an obvious increase in intense rainfall events. Consequent studies further demonstrated that significant increases in precipitation extremes had been found in southwest, northwest, and eastern China, while the significantly decreasing trends were found in central, northern and northeast China, even though there was little change in total precipitation for China as a whole. In addition, an abrupt change of the number of days with extreme precipitation and the percentage of precipitation extremes were found during late 1970s and early 1980s over China (Zhai et al. 2005; Wang and Zhou 2005; You et al. 2011; Zhang et al. 2008; Wang et al. 2013). From a regional perspective, many related studies were also conducted in terms of extreme precipitation events in Yellow-Huaihe and Yangtze-Huaihe Rivers Basins (Dong et al. 2011; Zhang et al. 2013), southwestern China (Li et al. 2012), Loess Plateau (Yan et al. 2014) and Xinjiang (Jiang et al. 2013), as well as other regions (Nie et al. 2012; Tian et al. 2012).

Shandong province, located in eastern China, is an important economic and agricultural province with high population density. Its agricultural production, especially the grain production, is directly related to the social stability and sustainable development (Jiang et al. 2008). Jiang et al. (2011) analyzed the spatial characteristics and temporal trends of extreme precipitation events in Shandong based on daily precipitation data of 18 meteorological stations during 1961–2008 by utilizing four indices, and reported that the rainfall frequency, annual precipitation amount and annual daily maximum amount of precipitation extremes showed weak decreasing trends, while the precipitation intensity exhibited non-significant trend but with larger fluctuations during this period. The latest research by Zhuo et al. (2014) investigated the diurnal cycle of summer rainfall in Shandong, and suggested that the spatial distribution of abnormal precipitation was related to the effects from complex terrain and local climate characteristics. However, a number of issues remain unanswered although great progress on precipitation extremes has been made in Shandong, as few studies focused on the variations in intense rainfall events and corresponding potential physical mechanisms simultaneously in Shandong. In fact, severe natural disasters induced by precipitation extremes have increased and resulted in huge economic losses in recent years. For instance, severe droughts occurred persistently in 2010, 2011 and 2012. Especially, the most severe drought in recent decades, in 2010, caused approximately 2.47 million hectares of field crops being subjected to varying degrees of drought, and drinking water problems to 4 million people and 47,200 livestock (http://www.chinadaily.com.cn/china/2010-12/29/content_11773288.htm). Therefore, comprehensive analyses in the variations and underlying causes of extreme precipitation events are very necessary and urgent to regional water resources management and secure agricultural production in Shandong.

The main objective of this study is to investigate the spatial and temporal variations in precipitation extremes during 1951–2011 in Shandong, and to obtain a better understanding of the regional characteristics in extreme precipitation and further explore the influence of large scale atmospheric circulation patterns on the changes in precipitation extremes. The rest of paper is organized as follows: Sect. 2 introduces the study area, data and precipitation indices as well as the methodology. Research results are analyzed in Sect. 3. And the discussion is presented in Sect. 4, followed by the conclusions in Sect. 5.

2 Data and methodology

2.1 Research area

Shandong is located in a coastal region in east China and over the lower reach of the Yellow River, roughly from 34°22′ to 38°15′ N and 114°19′ to 122°43′ E (Fig. 1). The geomorphologic patterns of Shandong includes center, south and east regions with mountainous and hilly areas, while western and northern regions that are part of the northwest Shandong plains formed by the alluviation of the Yellow River, which is also part of East China Great Plains (Fig. 1). In terms of the magnitude and distribution of annual rainfall and administrative boundaries, in this study Shandong is divided into three regions, from west to east: Western Shandong, Central Shandong and Jiaodong peninsula (Fig. 1). Moreover, Shandong lies in a complex monsoon climate region, where the atmospheric circulation system is complicated, with winter controlled by strong Mongolia cold anticyclones, summer affected by the Indian low pressure and western Pacific subtropical high pressure, and spring and autumn in the winter-summer circulation conversion period. Thus, Fig. 2 shows that great disparities appear between summer and winter for the spatial distribution of daily mean precipitation, although it decreases from the southeastern to northwestern Shandong in general. Correspondingly, the rainfall exhibits uneven spatial distribution and significant inter-annual variations in Shandong which is typical of characteristics of East Asian monsoon climate (Jiang et al. 2008). However, the summer monsoon is unstable in recent years (Wang et al. 2001), making meteorological disasters easy to occur frequently in this region. Overall, the spatial variations of precipitation in Shandong are distinctive owing to the complex patterns of climate system and geography as well as the influences from ocean in the east.

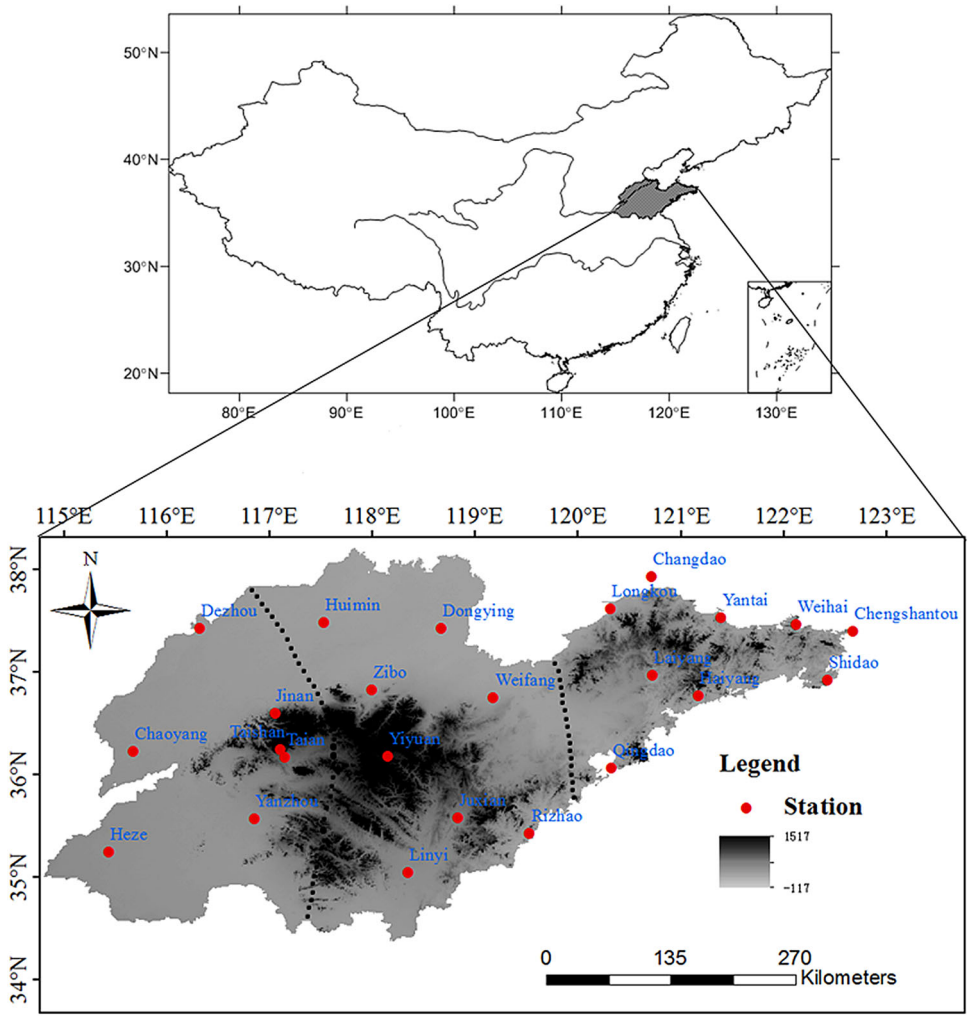

Fig. 1 The location of Shandong province in China and the distribution of rain gauging stations, and elevation is colored based on a Digital Elevation Model (DEM). Thick *dashed line* is split boundaries, from west to east: Western Shandong, Central Shandong and Jiaodong peninsula

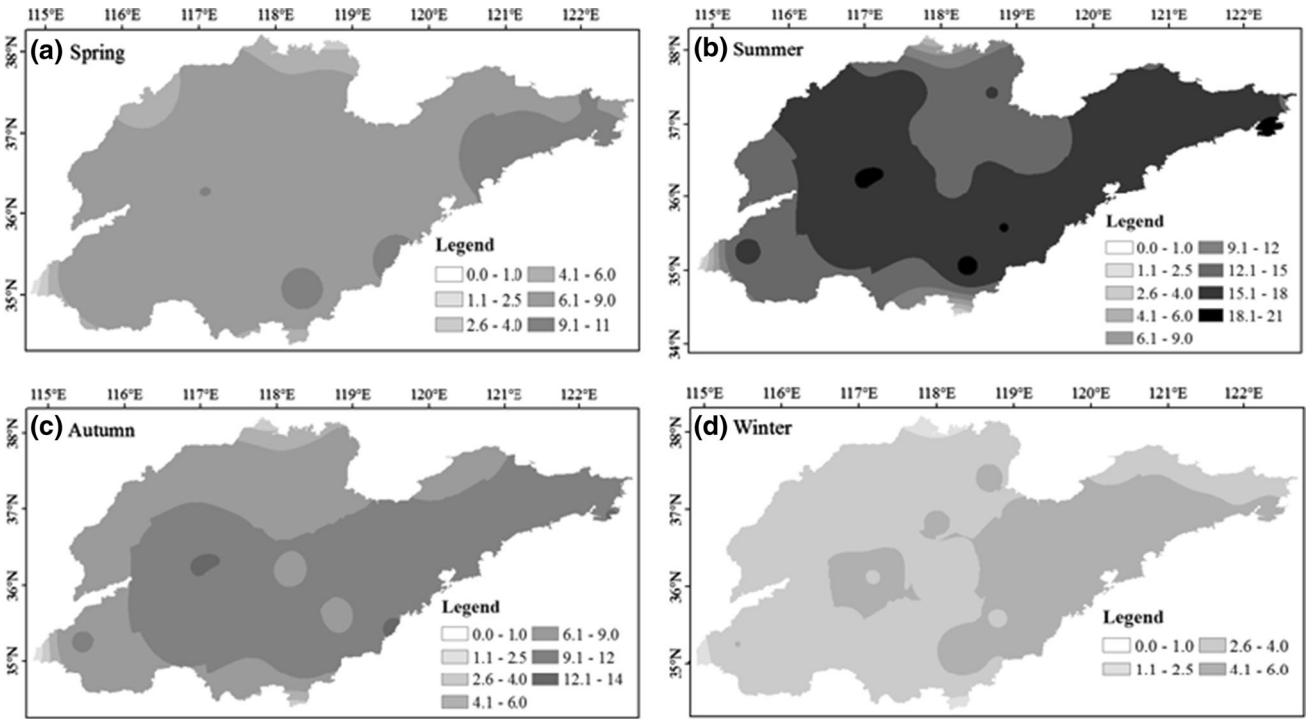

Fig. 2 Spatial distribution of daily mean precipitation in four seasons over the Shandong during 1971–2000

2.2 Data and indices

A dataset of daily precipitation amounts at 24 stations along with detailed metadata distributed evenly from January 1951 to December 2011 has been used in this study (Table 1). It includes almost all first-class national climate stations and reference stations in Shandong, which are developed at the Climate Data Center (CDC) of the China Meteorological Administration (CMA). Because the frequency, intensity and duration of extreme precipitation events are sensitive to the length of observation dataset and the erroneous outliers might impact trend analysis (Zhang et al. 2011), it is necessary to choose the length of the homogeneous record period and minimize the missing data before using the meteorological data in trend analysis. The modern nationwide network of weather observing stations in China began its operation in the 1950s, thus, 1951 is selected as the starting year in this study. A year is considered to be missing if there are more than 10 % missing days. A station is retained only if it has more than 43 non-missing years of data, while a station with poor quality and not-long enough period is rejected. Additionally, retaining useful data in data sparse areas is also a consideration. As a result, 24 stations meet these criteria and have data available for at least 43 year after data quality control and homogeneity assessment (Table 1). For further understanding of changing patterns in large scale atmospheric circulation, mean circulation composites of horizontal wind fields and geopotential height at 850 and 500 hPa from the National Centers for Environmental Prediction/National Center for Atmospheric Research (NCEP/NCAR) reanalysis data were analyzed (Kalnay et al. 1996).

Data quality control was performed by utilizing the computer program RClimDex, and the data homogeneity was assessed with the RHtest software (available from http://cccma.seos.uvic.ca/ETCCDI/software.shtml) (see Zhang and Yang 2004 for more details). In this study, the analyses of precipitation extremes are based on the 11 precipitation indices defined by STAtistical and Regional dynamical Downscaling of EXtremes for European regions (ETCCDMI), as listed in Table 2. These indices have been widely used in previous studies for measuring and monitoring extreme precipitation events (e.g., Alexander et al. 2006; Li et al. 2012; Powell and Keim 2014). The RClimDex program allows for one user-defined input when calculating precipitation indices, in this study the value of user-defined input is defined as 1-day precipitation $\geq$50 mm/day, which is in conjunction with the regulations of the CMA. Furthermore, The RClimDex program uses a bootstrapping technique to address discontinuities in the expected rates for the years on the boundaries of the base period, thereby making estimations of threshold exceedance rates for both the in-base and out-of-base periods comparable and temporally consistent (Zhang and Yang 2004; Zhang et al. 2005). Additionally, the RHtest software employs a two-phase regression model to check for multiple step change point that

Table 1 Detailed meteorological records of stations in Shandong

Name	Longitude	Latitude	Altitude (m)	Length (years)
Dezhou	116.32°E	37.43°N	21.2	46
Huimin	117.53°E	37.48°N	11.7	61
Dongying	118.67°E	37.43°N	6.0	54
Changdao	120.72°E	37.93°N	39.7	51
Longkou	120.32°E	37.62°N	4.8	55
Yantai	121.40°E	37.53°N	46.7	43
Weihai	122.13°E	37.47°N	65.4	52
Chengshantou	122.68°E	37.40°N	47.7	60
Chaoyang	115.67°E	36.23°N	37.8	55
Jinan	117.05°E	36.60°N	170.3	61
Taishan	117.10°E	36.25°N	1533.7	58
Taian	117.15°E	36.17°N	128.8	43
Zibo	118.00°E	36.83°N	34.0	46
Yiyuan	118.15°E	36.18°N	305.1	54
Weifang	119.18°E	36.75°N	22.2	61
Laiyang	120.73°E	36.97°N	54.4	57
Qingdao	120.33°E	36.07°N	76.0	51
Haiyang	121.18°E	36.77°N	40.9	53
Shidao	122.43°E	36.92°N	4.8	56
Heze	115.43°E	35.25°N	49.7	43
Yanzhou	116.85°E	35.57°N	51.7	61
Juxian	118.83°E	35.58°N	107.4	61
Linyi	118.35°E	35.05°N	87.9	49
Rizhao	119.53°E	35.43°N	36.9	57

could exist in a time series, with the purposes to identify potential inhomogeneities in the data.

2.3 Methodology

The simple linear regression method is utilized to analyze the long-term climatic trends of 11 precipitation indices among the 24 meteorological stations. The statistical significance of the trends is evaluated by the rank-based Mann–Kendall (MK) trend test (Mann 1945; Kendall 1970), this is a nonparametric method, and commonly used to assess the significance of monotonic trends in hydro-meteorological time series (Yue and Pilon 2004). The abrupt step changes and periodic oscillation of precipitation extremes are also studied for extreme precipitation in Shandong. From a statistical point of view, the time series of precipitation extremes is non-stationary (Mearns et al. 1984; Meehl et al. 2000). The Ensemble empirical mode decomposition (EEMD) has been widely used in the analysis of nonlinear and non-stationary data. Therefore, an EEMD analysis is applied to detect the inter-annual and decadal-scale variability of extreme precipitation in this study. The basic idea of EEMD is the decomposition of a time series into a finite set of intrinsic mode functions (IMFs) that admit a well-behaved Hilbert transform. Each mode describes the scale and energy characteristics at any time.

An arbitrary, real value time series, $f(t) = L^2(R)$, has Hilbert transform g(t)

Table 2 Definitions of 11 extreme precipitation indices used in this study

ID	Index name	Definition	Units
RX1day	Max 1-day precipitation	Annual maximum 1-day precipitation	mm
Rx5day	Max 5-day precipitation	Annual maximum consecutive 5-day precipitation	mm
R10	No. of heavy precipitation days	Annual count of days when precipitation ≥10 mm	Days
R20	No. of very heavy precipitation days	Annual count of days when precipitation ≥20 mm	Days
R*nn*	No. of days above *nn* mm	Annual count of days when precipitation ≥*nn* mm (user-defined threshold)	Days
SDII	Simple daily intensity index	Annual total precipitation divided by the number of wet days (precipitation ≥1.0 mm) in the year (Average precipitation on wet days)	mm/day
CDD	Consecutive dry days	Maximum number of consecutive days with precipitation < 1 mm	Days
CWD	Consecutive wet days	Maximum number of consecutive days with precipitation ≥1 mm	Days
R95p	Precipitation on very wet days	Annual total PRCP when precipitation >95th percentile of 1961–1990 daily precipitation	mm
R99p	Precipitation on extremely wet days	Annual total PRCP when precipitation >99th percentile of 1961–1990 daily precipitation	mm
PRCPTOT	Annual total wet day precipitation	Annual total precipitation in wet days (precipitation ≥1 mm)	mm

All indices are calculated by RClimDex. A wet day is defined when precipitation ≥1 mm, and a dry day when precipitation <1mm

$$g(t) = \frac{1}{\pi} P \int_{-\infty}^{+\infty} \frac{f(t')}{t - t'} dt' \quad (1)$$

where P is the Cauchy principal value. A unique analytic function $z(t)$ can be defined by the complex conjugate pair $f(t)$ and $g(t)$,

$$z(t) = f(t) + ig(t) = a(t)e^{i\theta(t)} \quad (2)$$

where $a(t)$ and $\theta(t)$ are the local amplitude and phase, respectively, defined by

$$a(t) = [f^2(t) + g^2(t)]^{1/2}, \ \theta(t) = \arctan\left[\frac{g(t)}{f(t)}\right], \quad (3)$$

From Eq. (3), the local or instantaneous frequency can be derived as

$$\omega = \frac{d\theta(t)}{dt}. \quad (4)$$

Compared to the EEMD method, traditional Fourier Analysis transfers the time series from the time domain to the frequency domain with constant amplitude and frequency, without any resolution in the time domain (Xie et al. 2002). Wavelet Analysis provides definite resolutions in both the time and frequency domains, and can also be used to study local structures of signals, but it cannot capture the physical mechanism while explaining a nonlinear phenomenon by adding non-existing harmonics. For EEMD, more detailed information is referred to Huang et al. (1998, 1999) and Huang and Wu (2008).

As demonstrated above, original data can be decomposed through EEMD analysis. Taking RX1day anomaly at Weihai station for example, the original data (Fig. 3a) is decomposed into 5 IMFs (Fig. 3b–f). Figure 3f should be the trend of original data, but in this example, this component may be excessively extracted, i.e. the curve is too smooth, while the sum of the latest IMFs may already satisfy the definition of a trend (Fig. 3g) (Huang and Wu 2008). Thus, this method, containing more physical meanings than ordinary moving average method, is adopted in this study. Moreover, the EEMD method with a 0.2 standard deviation for noise access and 100 ensembles is adopted in this study (see Huang and Wu 2008 for details).

3 Results

3.1 RX1day and RX5day

The spatial distribution of trends in the time series for annual maximum daily precipitation (RX1day) and annual maximum consecutive 5-day precipitation (RX5day) are shown in Fig. 4a, b. RX1day decreased in the southeast coast and west with several stations exhibiting statistically significant increasing trend in Central Shandong. RX5day showed a similar trend distribution as RX1day.

Linear trends of RX1day varied from −8.25 to 4.43 mm/decade, with a regional average of −0.9 mm/decade. The largest positive magnitude was discovered at Jinan station and the largest negative magnitude was found at Heze station in southwest Shandong. Downward trends were observed at 16 out of 24 stations (Table 3), it can be found from Fig. 4a that most of the stations were characterized by negative trend for the RX1day. Overall, southeast coast and southwest areas experienced a larger decreasing rate of the RX1day than southern and northern parts of the Shandong. Several stations, including Yiyuan, Linyi in Central Shandong and Changdao in the northeast Shandong, were dominated by relatively higher positive trends (Fig. 4a). MK significance test for the trends of the RX1day showed that 7 out of 24 stations have significant downward trends (at $p < 0.05$), accounting for 21.7 % of the stations with negative trends (Table 3). Figure 4a also illustrates that the distribution pattern of stations with significant MK upward trend is different from those stations exhibiting large negative trends, and most of the stations with significant upward trends were located in the Central and northwest Shandong.

The variations of trends mentioned above can also be observed in Fig. 5, which illustrates that average decreasing trends occurred in Jiaodong peninsula, Central Shandong and the entire Shandong, while the significant increasing trend was only observed in the western regions. The results of EEMD analysis indicated that the inter-annual and decadal variability of RX1day was detected in the entire Shandong and three sub-regions. In general, a slight long-term decrease from the 1960s to the early period of 1980s is present, and then followed by a persistent increasing trend until early 2000, nevertheless, a decreasing trend was found in the recent 10 years.

RX5day maintained a relatively similar spatial distribution of trends to RX1day but with different magnitudes (Fig. 4b). The linear trends of RX5day in Shandong varied between −11.71 and 0.55 mm/decade, with a regional average of −2.5 mm/decade. The highest positive trend appeared at the Jinan station in east of Western Shandong, and the largest negative trend was discovered at Taian station in east of Central Shandong. Geographically, Changdao is located in the junction of the Yellow Sea and Bohai Sea, and is the only island county in Shandong. Taian is near the Taishan Mountain being the highest elevation point in Shandong. It is apparent that RX5day may be influenced by marine and terrain to a certain extent. Generally, about 66.7 % of the stations had decreasing trends and these stations scattered in most parts of Shandong except for isolated stations in the central regions.

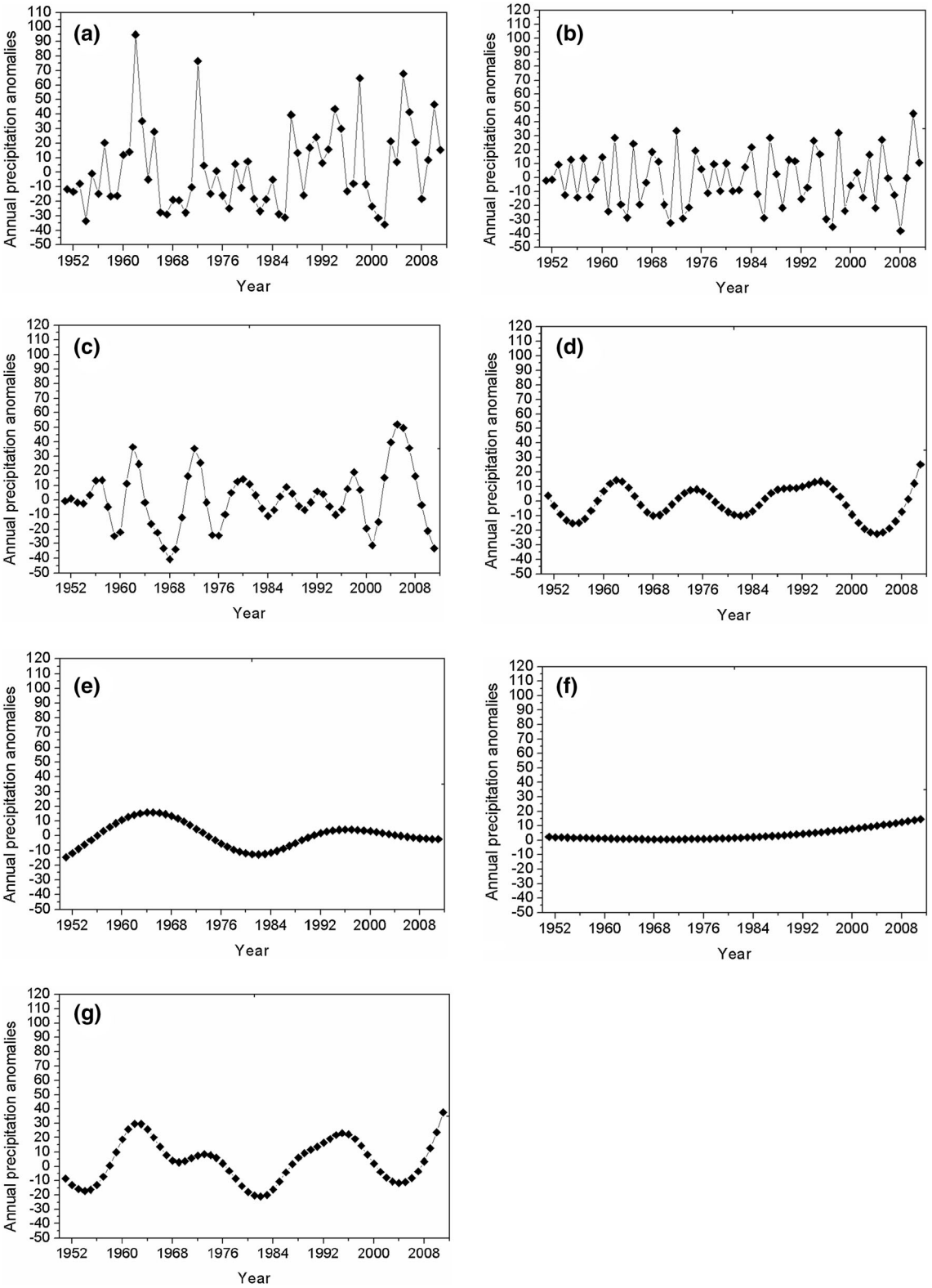

Fig. 3 Results of EEMD analysis for RX1 day anomaly at Weihai station, **a** denotes original input data, **b–f** denote IMFs of frequencies from high to low, respectively, **g** denotes the sum of the latest *columns* (the sum of **d–f**) of analysis results

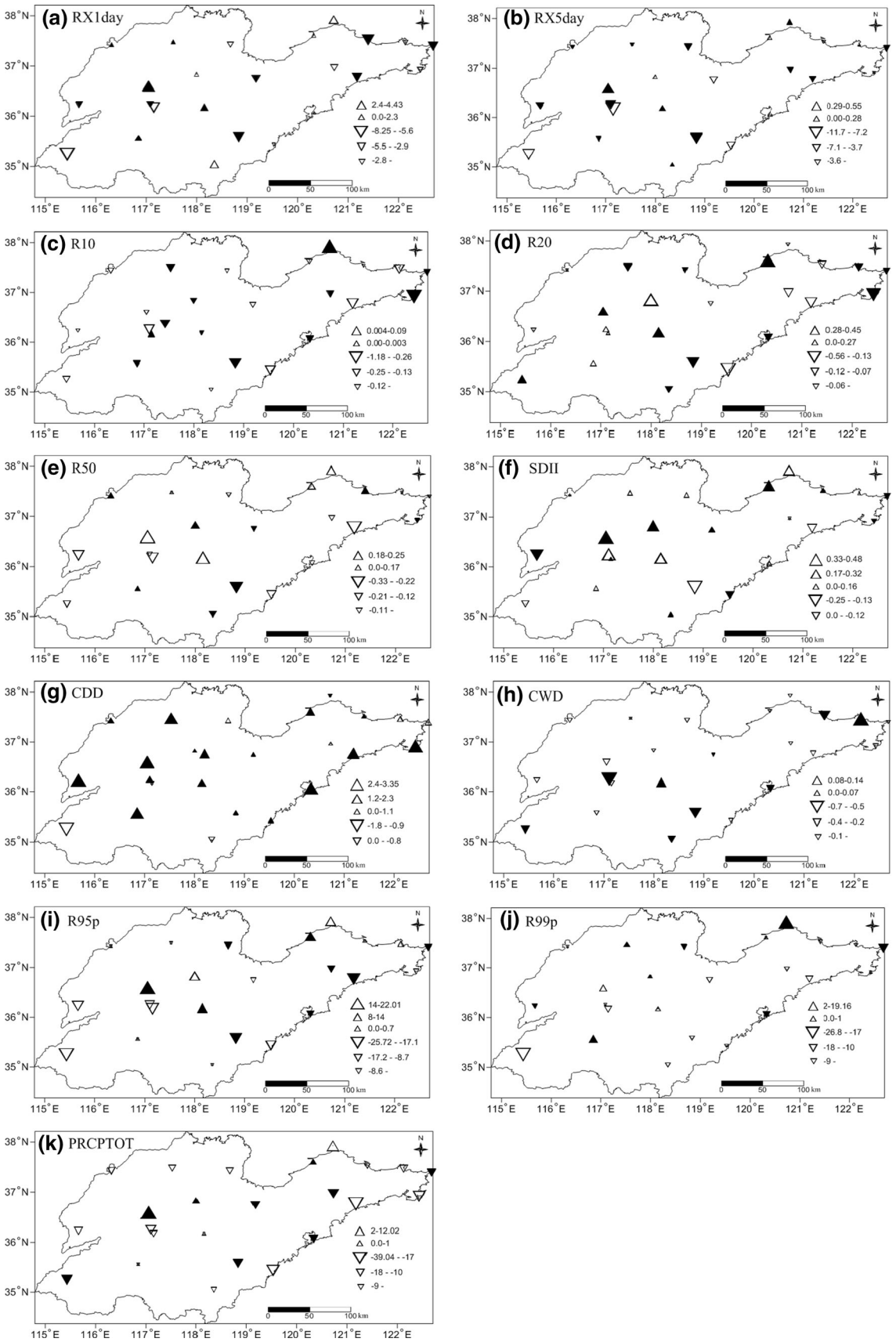
(a) RX1day
2.4-4.43
0.0-2.3
-8.25 - -5.6
-5.5 - -2.9
-2.8 -
(b) RX5day
0.29-0.55
0.00-0.28
-11.7 - -7.2
-7.1 - -3.7
-3.6 -
(c) R10
0.004-0.09
0.00-0.003
-1.18 - -0.26
-0.25 - -0.13
-0.12 -
(d) R20
0.28-0.45
0.0-0.27
-0.56 - -0.13
-0.12 - -0.07
-0.06 -
(e) R50
0.18-0.25
0.0-0.17
-0.33 - -0.22
-0.21 - -0.12
-0.11 -
(f) SDII
0.33-0.48
0.17-0.32
0.0-0.16
-0.25 - -0.13
0.0 - -0.12
(g) CDD
2.4-3.35
1.2-2.3
0.0-1.1
-1.8 - -0.9
0.0 - -0.8
(h) CWD
0.08-0.14
0.0-0.07
-0.7 - -0.5
-0.4 - -0.2
-0.1 -
(i) R95p
14-22.01
8-14
0.0-0.7
-25.72 - -17.1
-17.2 - -8.7
-8.6 -
(j) R99p
2-19.16
0.0-1
-26.8 - -17
-18 - -10
-9 -
(k) PRCPTOT
2-12.02
0.0-1
-39.04 - -17
-18 - -10
-9 -
38°N
37°N
36°N
35°N
115°E 116°E 117°E 118°E 119°E 120°E 121°E 122°E
0 50 100 km
N

◀**Fig. 4** Spatial distribution of trends for precipitation indcies. Positive trends are shown as *triangles*, negative trends as *inverted triangles*. Stations with significance of the trend by 95 % confidence level can be identified by *black triangles*

EEMD analysis revealed that the RX5day exhibited relatively larger fluctuations although non-significant decreasing trends were displayed (see Supplementary Fig. S1). A slight long-term decrease of the RX5day in the entire Shandong from the 1960s to the late 1970s and a roughly persistent increasing trend from the late 1970s to the mid-1990s were shown in Supplementary Fig. S1d.

3.2 R10, R20 and R50

The spatial distribution of linear trends of heavy (R10), heavier (R20) and heaviest precipitation days (R50) were similar but with different magnitudes (Fig. 4d–f). The same station frequently exhibited statistically significant increasing or decreasing trends with different indices for R10, R20 and R50. Three indices at most stations were characterized by downward regional trends but only the R10 was statistically significant (Table 3). The linear trends of the R10 in Shandong ranged between −1.18 and 0.09 days/decade, with a regional average of −0.3 days/decade. Decreasing trends were observed at 22 out of 24 stations, while only two stations, the Changdao and Taian in the east of Western Shandong, exhibited increasing trends (Table 3). The largest upward trend occurred in Changdao station, while the highest downward trend was observed at the Shidao station in the eastern Shandong with changing rate of 0.09 and −1.18 days/decade, respectively. Interestingly, two adjacent stations, Taian with altitude of 128.8 m and Taishan Mountain with altitude of 1533.7 m, experienced opposite trends, which may reflect the impacts of topography on precipitation.

The spatial distribution of linear trends of the R10 is illustrated in Fig. 3d. 22 stations covering most of the areas in Shandong had downward trends, and most of the stations exhibiting statistically significant trend with large magnitude were located along southeast coast. Statistically significant positive and negative trends are also shown in Fig. 3d. 40.9 % of the stations have significant downward trends (Table 3), and these downward trends in R10 can also be seen in Fig. 6. Negative linear trends were detected in three sub-regions and entire Shandong, but there are large fluctuations in EEMD results in Central and entire Shandong. Figure 6d also indicates the presence of a weak long-term decrease from 1960s to the early period of 1970s and then a roughly persistent increasing trend of the R10 starting from the early-1980s in Shandong. In addition, a quasi-decadal oscillation was also illustrated in Fig. 6.

The linear trends of R20 varied between −0.56 and 0.45 days/decade, with a regional average of −0.04 days/decade. Downward trends were observed at 14 out of 24 stations, and the stations with negative trends were located in east, southeast coast and northern Shandong, while those with upward trends were located in mid-south and southwest Shandong (Fig. 4e). A slightly positive linear trend was detected in Western Shandong, and negative trends were investigated in Central Shandong and Jiaodong peninsula (see Supplementary Fig. S2a). The results of EEMD analysis indicated a weak long-term decrease of the R20 in the entire Shandong from the 1970s to the early-1980s and a roughly persistent increasing trend from the mid-1980s to the mid-1990s.

Table 3 Trends per decade and percentage of stations with positives or negative trends for regional indices of extreme precipitation events in Shandong

Index	Regional trends	Range	Percentage of stations with upward trend	Percentage of stations with significant upward trend	Percentage of stations with downward trend	Percentage of stations with significant downward trend
RX1day	−0.9	−8.25 to 4.43			70.8	21.7
RX5day	**−2.5**	−11.71 to 0.55			66.7	34.7
R10	**−0.3**	−1.18 to 0.09			91.7	40.9
R20	−0.04	−0.56 to 0.45			66.7	35.5
R50	−0.05	−0.33 to 0.25			62.5	19.7
SDII	0.1	−0.25 to 0.48	70.8	27.8		
CDD	**1.6**	−1.8 to 3.35	83.3	75		
CWD	**−0.1**	−0.7 to 0.14			91.7	26.7
R95p	−1.4	−25.72 to 22.01			58.3	31.3
R99p	−0.2	−26.08 to 19.16			62.5	18.8
PRCPTOT	**−9.4**	−39.04 to 12.02			79.2	42.3

[a] Bold indicates value for trends significance at 5 % level

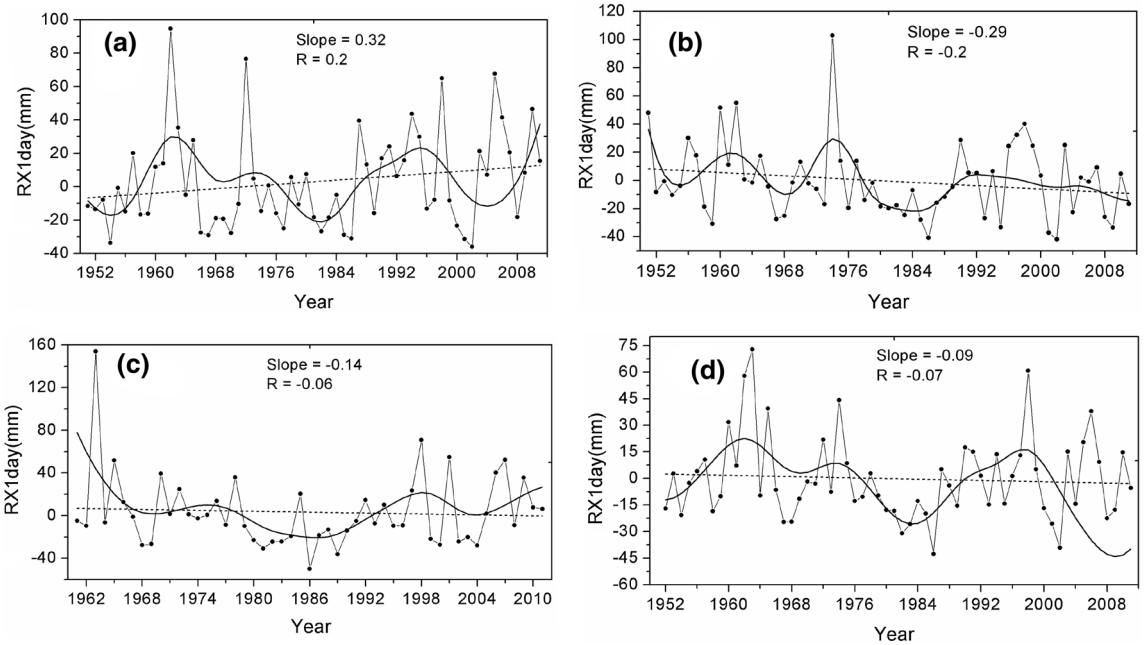

Fig. 5 Regional annual anomaly series of annual maximum 1-day precipitation (RX1 day) in **a** Western Shandong, **b** Central Shandong, **c** Jiaodong peninsula and **d** entire Shandong. The *dot line* is the linear trend and R is its correlation coefficient. *Slope* indicates trend per year, and the *slope* in *bold* indicates trend significance exceed the 95 % confidence level. The *smoother line* is the results of EEMD analysis and the *solid line* with *dots* is the original annual anomaly series

The linear trends of R50 ranged between −0.33 and 0.25 days/decade, with a regional average of −0.05 days/decade, and negative trends were observed at 15 out of 24 stations. The variations of R50 were inconsistent with ones for R10 and R20, whereas an upward trend was seen at 9 stations covering the east of Western Shandong and northeast regions. The highest upward trend occurred at Jinan station, while the largest downward trend was observed at Haiyang station in the southeast regions (Fig. 4f). The west region experienced a significant positive linear trend with large fluctuations, while the linear trend was not significant for entire Shandong. From the

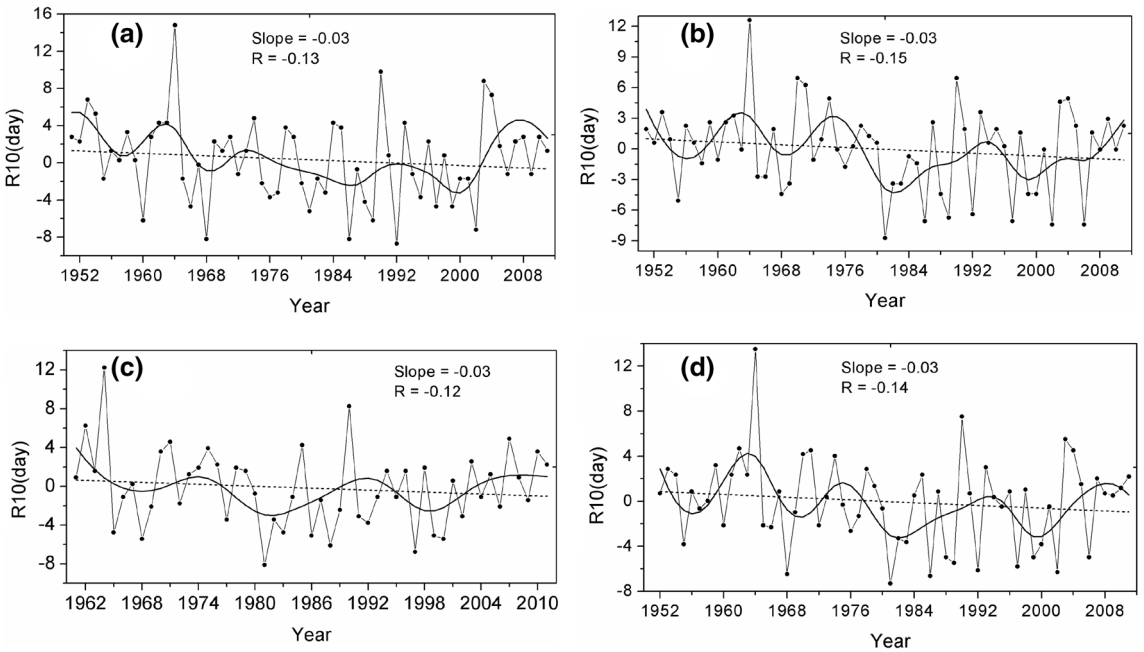

Fig. 6 The same as Fig. 5, but for annual count of days when precipitation ≥10 mm (R10)

spatial distribution perspective, changing trends and magnitudes of R50 are similar to RX1day and RX5day (see Supplementary Fig. S3). Thus, it can be concluded that the variability of RX1day and RX5day play a crucial role in the variations of R50 to some extent.

3.3 SDII, CDD and CWD

The linear trends of SDII ranged between −0.25 and 0.48 mm/decade, with a regional average of 0.1 mm/decade. Upward trends were detected at 17 out of 24 stations, while other 6 stations exhibited downward trend and one station had no trend (Table 3). The highest upward trend occurred at Jinan station in the east of Western Shandong, while the largest downward trend was observed at the Juxian station in the south of Central Shandong. Several stations with statistically significant positive trends were mainly located in Central Shandong and the northeast regions, this is roughly similar to the spatial distribution of R20 (Fig. 4c, e). MK significance testing for the trends of the time series for SDII showed that 27.8 % of the stations have significant upward trends (at $p < 0.05$). Figure 7 shows the long-term variation of the SDII for the entire Shandong and its three sub-regions. Western Shandong and Jiaodong peninsula displayed a significant increasing trend with small fluctuations, however, large fluctuations were detected in the latest 10 years in Western Shandong (Fig. 7a, c). The trend was not significant but large fluctuations were detected in Central Shandong, and for the entire Shandong, there was a roughly persistent increasing trend of the SDII since the early 1980s.

Linear trends of the CDD in Shandong varied between −1.8 and 3.35 days/decade, with a regional average of 0.16 days/decade. Upward trends were observed at 20 out of 24 stations with other 4 stations exhibiting a downward trend (Table 3). The highest upward trend occurred at Chaoyang station, while the largest downward trend was observed at the Heze station in the southwest region. The magnitude of the positive trends decreased from west to east, but three stations with significantly positive trends were found in the southeast region (Fig. 4g). MK significance testing for the trends in the time series of CDD demonstrated that 75 % of stations had significant upward trends (at $p < 0.05$), and these stations were mainly located in the Central and northern parts of Shandong. Above-mentioned upward trends of the CDD can also be detected in Fig. 8. All the three sub-regions and the entire Shandong showed a significant upward trend while the Western and Central Shandong experienced large fluctuations. A slight long-term decrease was observed from the 1970s to the early 2000, followed by a small increasing trend after 2004. The significant upward trend for CDD indicates that drought severity has increased, and severe droughts that occurred in consecutive years recently in Shandong were consistent with the variability of CDD in this period. This is also in agreement with previous studies focusing on droughts in China (Zou et al. 2005; She and Xia 2013).

The linear trends and spatial distributions of CWD are roughly opposite to those for CDD (Fig. 4g, h), which is clearly understood because an increase of consecutive dry days would result in a decrease of consecutive wet days. Compared to the general increasing trends for CDD in Fig. 8, the linear trends were decreasing, and the trends in recent years were also decreasing (see Supplementary Fig. S4). If this trend persists, Shandong would experience more droughts in the coming years.

3.4 R95p, R99p and PRCPTOT

The spatial characteristics and trends are similar between R95p and R99p, but with different magnitudes (Fig. 4i, j). The linear trends of R95p ranged between −25.72 and 22.01 mm/decade, with a regional average of −0.14 mm/decade, the downward trends were observed at 14 out of 24 stations (Table 3). Several stations characterized by positive trends were distributed in Central Shandong and the northeast regions, while the stations with negative trends are detected in the southeast coast region and Western Shandong (Fig. 4i). From R99p, it can be seen that the linear trends varied between −26.08 and 19.16 mm/decade, with a regional average of −0.02 mm/decade, downward trends were observed at 16 out of 24 stations, with 8 stations exhibiting upward trends (Table 3). The largest downward trend occurred at Heze station, while the highest upward trend was observed at the Changdao. Western Shandong displayed significant increasing trends for R95p and R99p with large fluctuations (Fig. 9a and Supplementary Fig. S5a). Central Shandong experienced a weak average decreasing trend for the two indices and also with large fluctuations (Fig. 9b and Supplementary Fig. S5b).

The PRCPTOT also had complicated trends, but its spatial pattern is consistent with those for R95p, R50 and RX1 day (Fig. 4a, e, i, k). A downward trend was observed at 18 out of 24 stations and mainly located in the mid-east regions and Western Shandong, while 6 stations located in the central and northeast parts of Shandong showed upward trends (Fig. 4k). The linear trends varied between −39.04 and 12.02 mm/decade, with a regional average of −0.94 mm/decade (Table 3). On the whole, a statistically significant decreasing linear trend was discovered for PRCPTOT from the 1950s to present and the fluctuation was also large (Fig. 10d). This is likely associated with the significant increasing trend of CDD. In the three sub-regions, negative trends were detected in Central Shandong and Jiaodong peninsula, while a small increasing trend was displayed in Western Shandong. Figure 10d indicated a slight long-term decrease from the 1960s

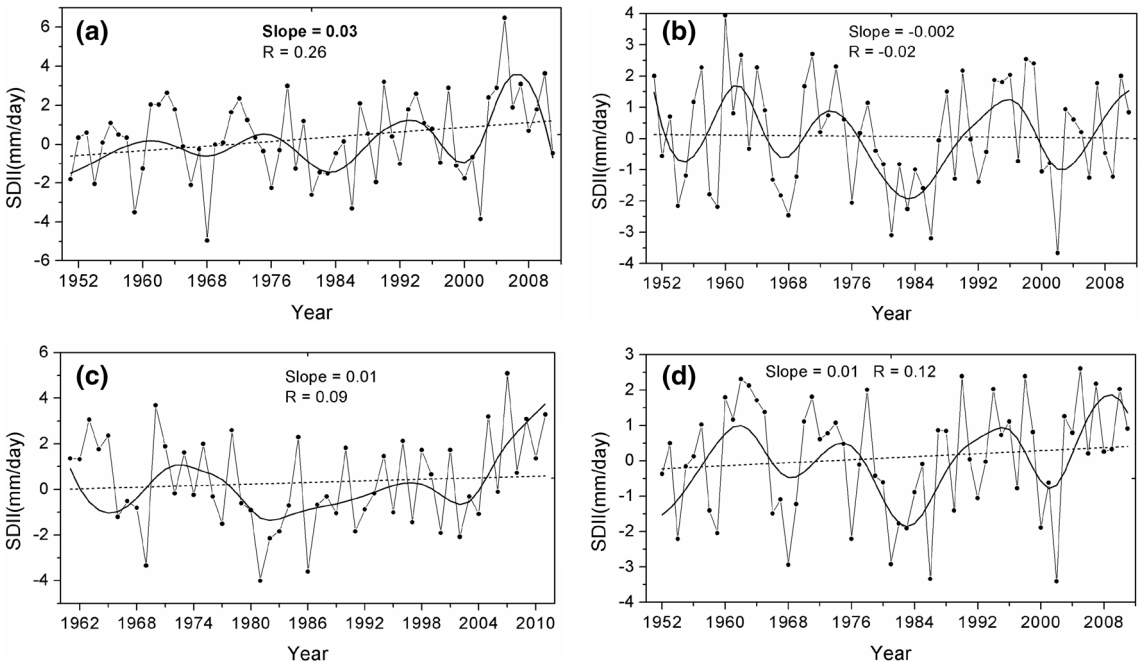

Fig. 7 Same as Fig. 5, but for simple daily intensity index (SDII)

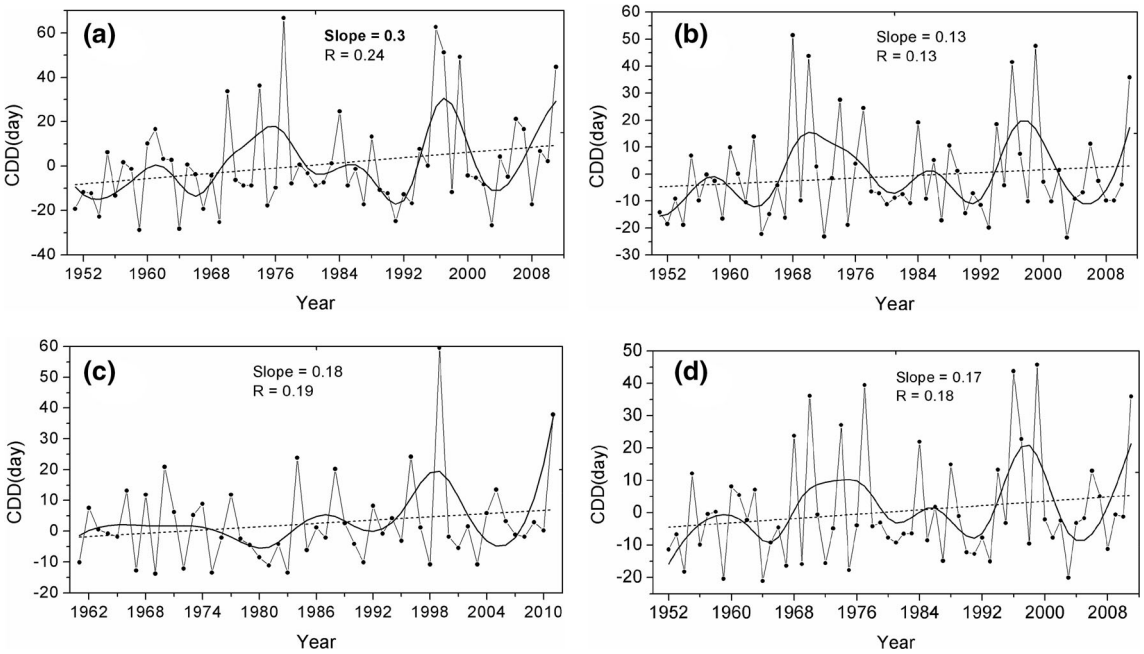

Fig. 8 Same as Fig. 5, but for maximum number of consecutive days with precipitation <1 mm (CDD)

to the 2000s and the oscillation period of 10–15 years was revealed in PRCPTOT.

3.5 Seasonal trends for RX1day and RX5day

To further investigate the precipitation trends in Shandong, RX1day and RX5day are selected to conduct seasonal analyses (Fig. 11). These two indices are chosen as they are able to better characterize the regional precipitation features (Alexander et al. 2006). It can be seen that trends are generally similar between summer and annual scales for these two indices, and the decreasing trends are dominant and mainly distributed over southeast coast, Central Shandong and southwestern regions (Figs. 4a, b, 11, 4a, b).

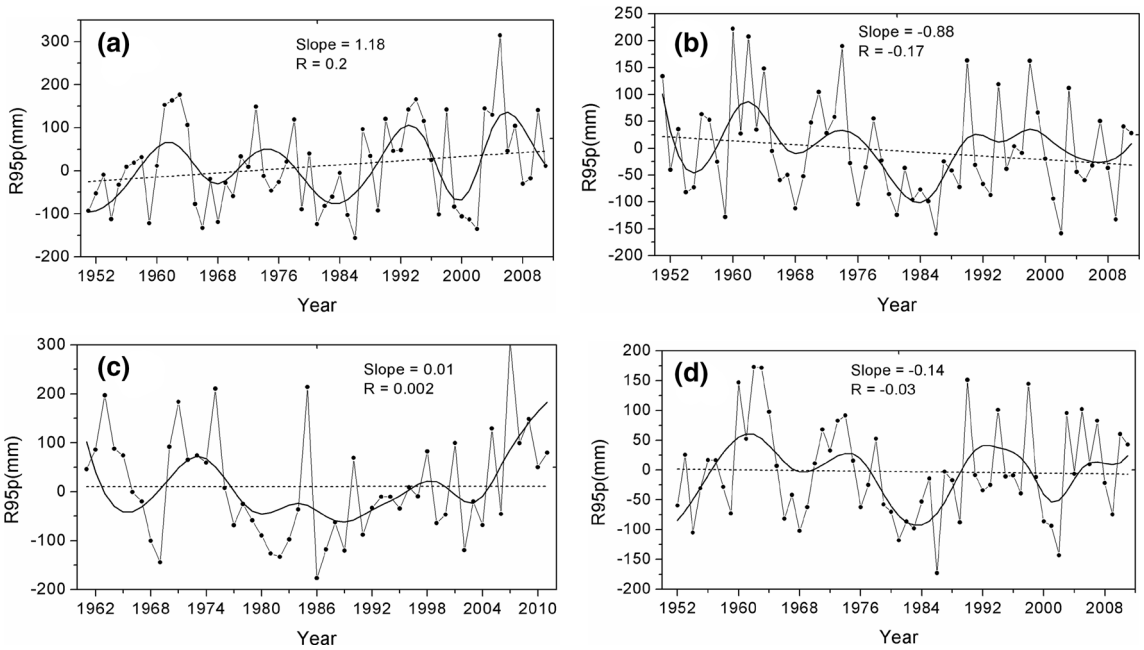

Fig. 9 Same as Fig. 5, but for very wet days (R95p)

The variations in winter are distinctive compared with ones in summer, particularly, more than half of the stations present increasing trends (Fig. 11). However, it's worth noting that the changes at Changdao station in the northeast Shandong exhibit significant trends in comparison with adjacent stations in all four seasons, and this is consistent with annual trends.

3.6 Linkage between extreme precipitation and annual total rainfall

A close linkage between the variations in extreme and total precipitation has been reported in many regions. Zhai et al. (2005) indicated that the extreme precipitation (R95p and R99p) typically accounts for 30–40 % of annual totals

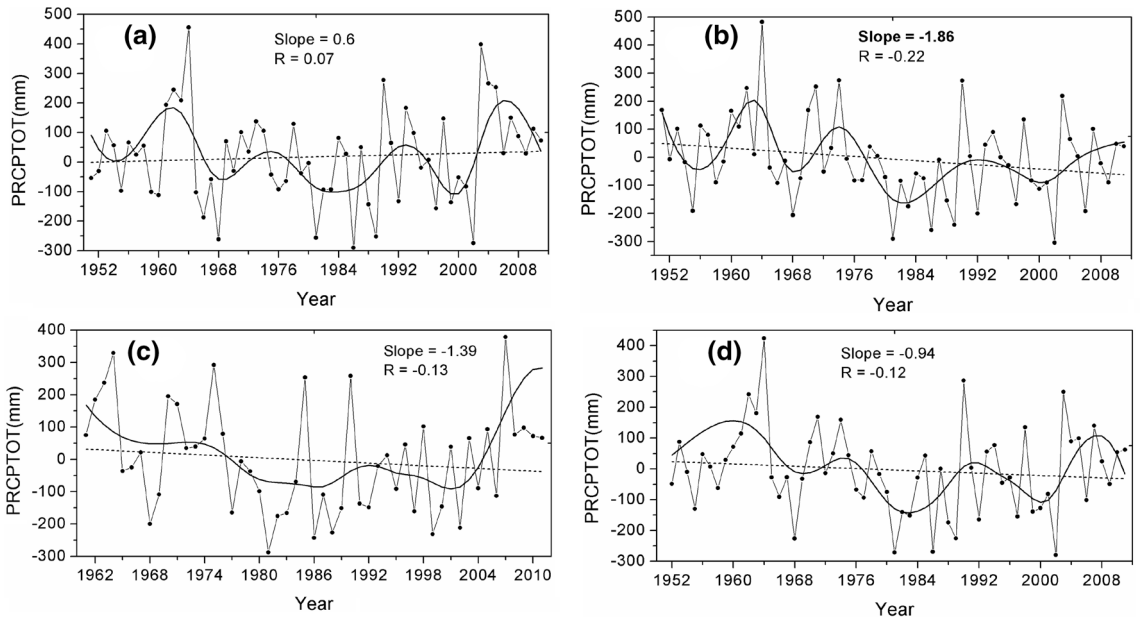

Fig. 10 Same as Fig. 5, but for annual total precipitation in wet days with precipitation ≥1mm (PRCPTOT)

across China. Liu et al. (2005) also reported that 95 % of the increase of total precipitation in China during 1960-2000 was contributed by the increased frequency of precipitation extremes. In fact, the spatial distribution of the precipitation indices in this study also indicated a close similarity between the precipitation extremes and the total precipitation (Fig. 4). However, the contribution of extreme precipitation to total rainfall only increased in Western Shandong during 1951–2011 (Fig. 12 and Supplementary Fig. S6). In other sub-regions and the entire Shandong, the contribution ratios had no-significant trend, but with large variations in their annual anomalies. The R95p approximately accounts for 25–30 % of annual total precipitation, while for R99p, the contribution is 6–16 %, and these ratios are slightly different from those found in other regions in China (Li et al. 2012; Yan et al. 2014). As demonstrated in Sect. 2, the rainfall in Shandong is mainly influenced by the East Asian summer monsoon (EASM) system. The prevailing causes for the changes of ratios may be that the EASM system is becoming more unstable or weaker in recent decades (Wang 2001; Gong and Ho 2003; Yancheva et al. 2007). In addition, the marine environment is likely to play a significant role on the variations in extreme precipitation over Jiaodong peninsula.

3.7 Changes in large scale atmospheric circulation

The possible mechanisms behind variations in extreme precipitation events in Shandong have been explored by analyzing the association of changing patterns of extreme precipitation with large scale atmospheric circulation on the basis of NCEP/NCAR reanalysis data. Earlier analysis results of extreme precipitation trends indicate that trend shift in the 1980s, so the averaged circulation maps in summer and annual scale are created for 1951–1980 and 1981–2011, and the former are subtracted from the latter (new minus old) to represent the variations in circulation between the two periods (Fig. 13). These seasons are chosen because heavy rainfall in Shandong mainly concentrates in summer.

Figure 13 shows the anomaly of wind vectors and geopotential height at 850 hPa between 1951–1980 and 1981–2011 at summer and annual scale. An obvious southward wind component is illustrated in Fig. 13a, which indicates a weaker EASM during 1981–2011 in comparison with that during 1951–1980. The southwesterly wind in eastern and northern China has weakened, and this will weaken the northward extension of the summer monsoon and limit the southwesterly summer monsoon flow to north China. The geopotential height composite shows that enhanced anticyclonic circulation has developed over the Eurasian continent, the largest differences appear near Mongolia and Lake Baikal (Fig. 13a). This significant increasing trend in geopotential height in northern regions will generate negative influences on the northward propagation of water vapor flux from the ocean, and lead to a longer rainy season in southern China and a shorter rainy duration in northern China. The changes in atmospheric

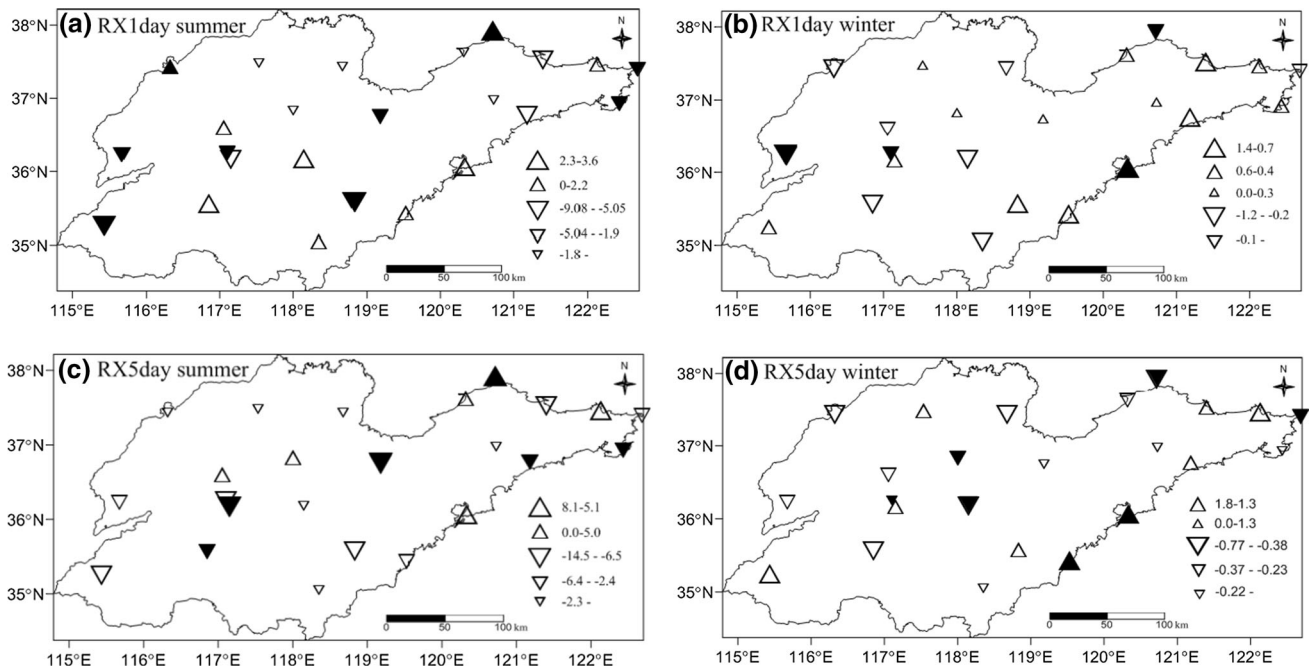

Fig. 11 Same as Fig. 4, but for summer and winter for indices of *RX1day* and *RX5day*, respectively

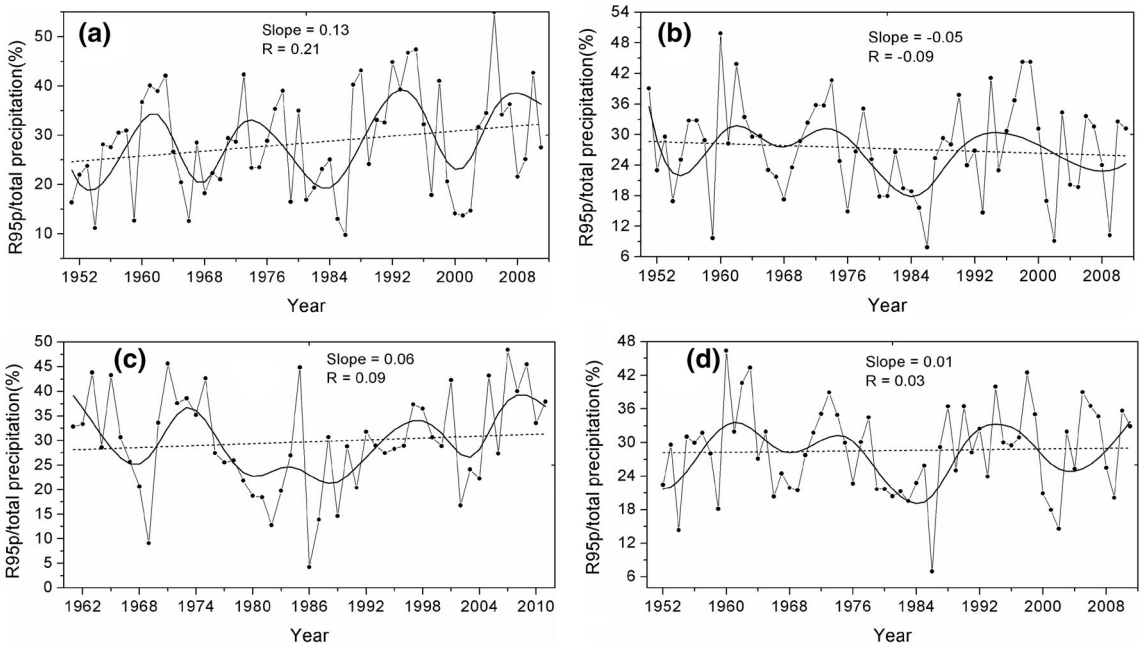

Fig. 12 Same as Fig. 5, but for regional series for the ratio of R95p to total precipitation

circulation patterns on annual scale are consistent with composites in summer (Fig. 13b). Simultaneously, the similar characteristics of wind fields and geopotential height are shown at 500 hPa (Supplementary Fig. S7).

To further diagnose changes in the circulations, composite analysis is also conducted in summer based on the variations for RX5day during 1964–1991. This period is selected because there are no missing data in the peninsula. RX5day could be linked to changes in atmospheric circulation (Mishra and Singh 2010), and it is chosen in this study. The ten biggest RX5day years (namely 1964, 1965, 1970, 1971, 1972, 1974, 1975, 1976, 1978, 1985) and ten lightest years (1969, 1980, 1981, 1983, 1984, 1986, 1987, 1988, 1989, 1990) are selected and small minus big computed to analyze the causes leading to decreasing rainfall trends (Fig. 14). Figure 14 illustrates that the changes in wind fields and geopotential height are also generally similar to those in Fig. 13a. This reconfirms our above analyses in changes of circulation. These would explain why a decreasing trend in amount and intensity of precipitation and an increasing for CDD occurred during recent decades in Shandong.

4 Discussions

Alexander et al. (2006) reported that extreme precipitation events in many mid-latitude regions were likely to increase, and the total area affected by drought since the 1970s has also increased. Nevertheless, Kunkel et al. (2003) and Wang et al. (2008) also showed general increasing trends in extreme climate events at a large spatial scale, but also suggested that the trends in particular regions were not conclusive, especially for precipitation extremes. Shandong is located in the mid-latitude in the Northern Hemisphere, and few studies were conducted with respect to extreme precipitation events in this region. The results in this study indicated that many precipitation indices, including RX5day, R10, CWD and PRCPTOT, were generally characterized by statistically significant decreasing trends. In addition, the trends for precipitation on very (or extremely) wet days also decreased. The SDII showed a weak positive trend, but it was not significant. Overall, the drought index CDD experienced a statistically significant increasing trend, which might have resulted from the reduction of rainfall over Shandong in recent years. However, the projected changes in precipitation by the CMIP5 (Coupled Model Intercomparison Project phase 5) multimodel ensemble suggests that extreme precipitation events, particularly for RX1day and RX5day, are projected to increase under the RCP4.5 and RCP8.5 emission scenarios by the end of the twenty-first century over north China, including Shandong (Zhou et al. 2014). This would be a good news for Shandong, where severe droughts occurred in recent years and wet indices decreased based on the rain gauge stations. Nevertheless, most regions of China, particularly for southern China, will become drier as described by the Palmer Drought Severity Index derived from CMIP5 models although the projected precipitation increases (Wang and Chen 2014). These may reflect possible future changes in circulations, especially for the East Asian Monsoon. It is worth noting that the

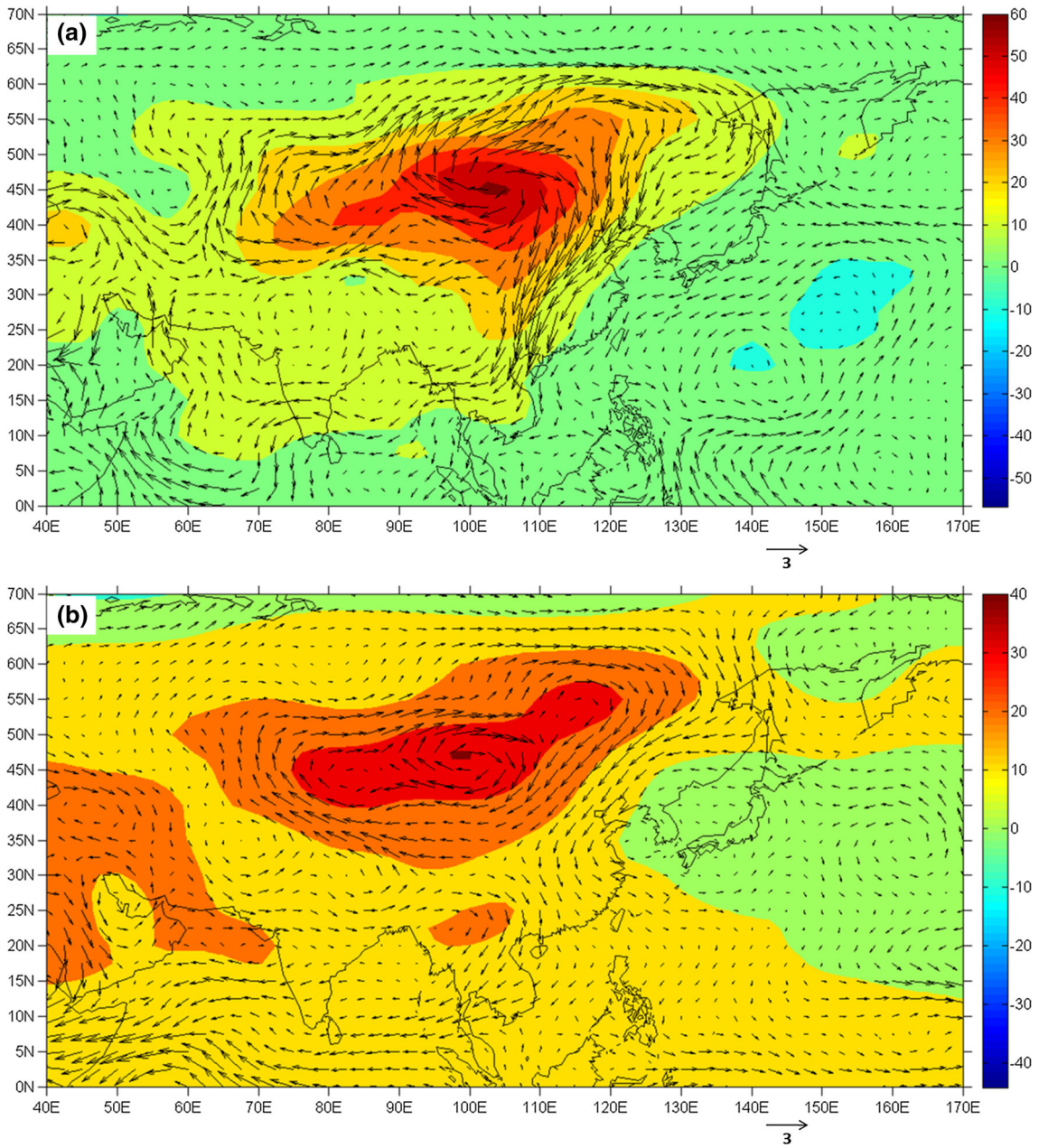

Fig. 13 Difference of *horizontal* wind (*vector*) and geopotential height (*shaded*) between 1951–1980 and 1981–2011 in summer (**a**), and annual scale (**b**) at 850 hPa

uncertainty in climate models would contribute to the uncertainty in the rainfall projections, resulting in a lack of ability for models at simulating intense precipitation at regional scales. As study by Chen and Frauenfeld (2014) reported that CMIP5 models overestimated the magnitude of seasonal and annual precipitation in most regions of China.

Precipitation intensity exhibited significant increasing trends over many regions in China (Zhai et al. 2005), and the increasing trend of SDII in Shandong was also associated with trends in national-scale, although just 27.8 % of the stations passed the significance test. In addition, a significant negative trend in intense rainfall was discovered in the mid- to lower reaches of the Yellow River (Dong et al. 2011). Thus, the increasing trends for droughts in Shandong was also with historical severe drought records in similar regions as well as the continued increase in the number of days drying-up (zero streamflow) episodes in lower reach of the Yellow River (Zou et al. 2005).

The indices of RX5day, R95p and PRCPTOT were dominated by consistent trends from east to west. However, the stations in Central Shandong, for example Jinan, Taian

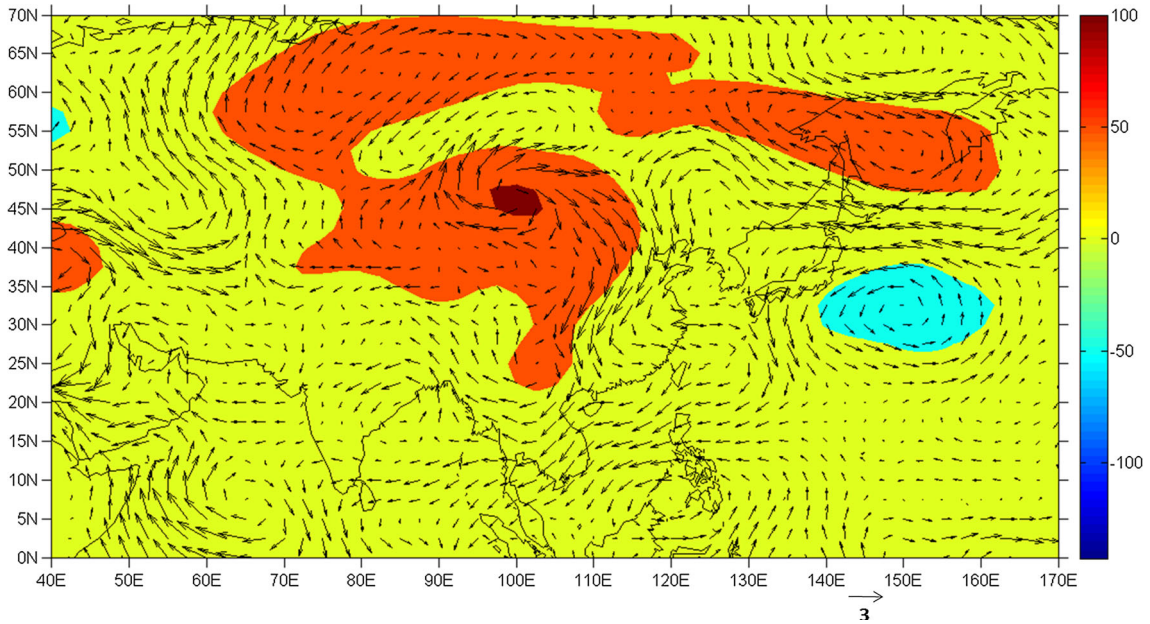

Fig. 14 Horizontal wind (*vector*) and geopotential height (*shaded*) between the average of ten heaviest years and ten lightest years, based on the changes for RX5day, at 850 hPa in summer

and Taishan Mountain, often exhibited opposite trends compared with the eastern and western regions of Mount Taishan. This was in keeping with Jiang et al. (2011), whose results also emphasized the variations in precipitation extremes in Central Shandong. In the present study, particularly for Jinan station, situated in the eastern side of Western Shandong, different or even opposite trends compared with the other stations in Central Shandong were found (Fig. 4). The causes may be that water vapor flux transported from the southeast oceanic regions is barred by Taishan Mountain, which leads to a significant effect on precipitation at Jinan, a station located on the inland side of the Taishan Mountain. Furthermore, Changdao, the only station surrounded by the sea in Shandong, often had different trends than the adjacent stations for the same precipitation index. These results indicated that topographic conditions and the influence of the ocean can lead to distinct trends in precipitation extremes.

The similarities of variations in extreme precipitation events and annual total rainfall were discovered in Shandong. Likewise, Dong et al. (2011) demonstrated that trends of extreme precipitation events were in good agreement with the variations of annual total precipitation in northern China. However, the increasing contribution made by extreme precipitation to annual total precipitation was only detected in Western Shandong. Other regions and entire Shandong had non-significant trends, this was different from the trends for above normal rainfall in some other regions over the world (Alexander et al. 2006). Interestingly, some changes in the characteristics of extreme indices, for example decreasing trends of RX5day, R95p PRCPTOT in Shandong, were also different from other conclusions (Jiang et al. 2013; Nie et al. 2012; Tian et al. 2012). The potential reasons are very complicated. Two distinct causes may be the differences in length of the rainfall time series and the spatial domains selected in different studies.

The potential physical mechanisms under the variations in precipitation extremes in Shandong might be that the weakened EASM limited northward transportation of water vapor flux from southeast oceans to northern China (Wang et al. 2001; Gong and Ho 2003). This decline of the EASM has contributed to more floods in southern China and severe droughts in northern China (Ding et al. 2009). The enhanced geopotential height over northern China and Mongolia has prevented northward transportation of water vapor flux, causing the longer stay of rainfall belt over the south, and limiting moisture propagation to the far north regions. These characteristics of circulation patterns may explain the changes in extreme precipitation indices and prolonged CDD in Shandong. Additionally, in-depth analysis of the physical causes of decline in EASM strength is beyond the scope of this study, this will be explored in our subsequent research.

5 Conclusions

Comprehensive analyses were conducted for the trends of extreme precipitation events and total rainfall during 1951–2011 from 24 selected stations in Shandong. An ensemble empirical mode decomposition (EEMD) analysis

is applied to investigate the periodic cycle of precipitation extremes. And the possible association with large-scale atmospheric circulation is also explored. The main conclusions are summarized below.

(1) In general, most rainfall indices in this study were characterized by decreasing trends except SDII and CDD. Specifically, CDD which represents drought conditions showed a statistically significant increasing trend at most stations in Shandong, and the magnitudes are larger in mid-west Shandong and southeast coast than elsewhere. The decreases in precipitation and increases in consecutive dry days inevitably lead to increases in droughts or severe droughts in Shandong. If the current trends continue, Shandong would experience more severe droughts in the coming years.

(2) Consistent reduction in the indices of RX5day, R95p and PRCPTOT demonstrated that extreme precipitation and total rainfall were all decreasing in Shandong except the Changdao station surround by the sea. Furthermore, the variations of CDD at the Changdao station were also inconsistent with the stations located in other parts of Shandong. These indicated that the marine environment may have significant influences on precipitation.

(3) Analysis of impact factors that have obvious effects on regional heavy precipitation is a complex process (Lea et al. 2000; Araújo et al. 2005). For example, RX5day, R95p and PRCPTOT showed decreasing trends from southeast coast to Western Shandong with the exception of a small number of stations in Central Shandong, where the influence from Taishan Mountain is evident. This revealed that the effects of topography were significant.

(4) Periodic oscillations of extreme precipitation indices were depicted by EEMD analysis. Most of the indices were characterized by large inter-annual and decadal fluctuations with the presence of a shift for trend in the 1980s, this similar trend shift in the 1980s was also found in other studies in eastern China (e.g., Gong and Ho 2002).

(5) Large-scale atmospheric circulation analysis indicates there was a weak EASM during 1981–2011 as compared to 1951–1980, but this needs to be investigated further. Enhancement of northeasterly wind prevents the northward transportation of water vapor flux and results in decreases in amount and intensity as well as duration of rainfall and an increase for CDD in Shandong. And the increasing geopotential height over the Eurasian continent confirms the changing circulation patterns in the above analysis.

Overall, there are significant spatial and temporal variability in the extreme and total precipitation in Shandong, which is associated with the changes of wet and drought patterns in the region. Thus, positive measures should be taken to alleviate disaster losses induced by precipitation extremes and ensure food security as well as socio-economic sustainable development. Moreover, taking into account the adverse trends of precipitation extremes at Changdao station surrounded by the sea, the analysis of physical mechanisms of extreme precipitation in Shandong from the point of view of air-sea interaction is a meaningful topic for future studies. Additionally, it should be noted that it is crucial to assess the field significance of the trends such as those presented in this study (Livezey and Chen 1983). However, the analysis of the field significance of the trends is not trivial (Villarini et al. 2013), and is beyond the scope of the present study. It will form the basis of our future study which focuses on the physical mechanisms for the variations in precipitation extremes and the co-variates in Shandong.

Acknowledgments We are heartily grateful to two anonymous reviewers, because their comments significantly improved this paper. This study is supported by the Taishan Scholar Fund (No. 3000-841112013) awarded by Shandong Province, National Natural Science Foundation of China (No. 41210008; No. 41275050), Shandong Natural Science Foundation (No. ZR2015DQ004), Young Academic Backbone and PhD Research Fund as well as Culture Research Center of lower reaches of Yellow River in Heze University. We also thank He Meng and Xiang Gong in Ocean University of China for providing useful suggestions.

References

Alexander LV, Zhang X, Peterson TC, Caesar J, Gleason B, Klein Tank A, Haylock M, Collins D, Trewin B, Rahimzadeh F (2006) Global observed changes in daily climate extremes of temperature and precipitation. J Geophys Res 111:D05109

Araújo MB, Pearson RG, Thuiller W, Erhard M (2005) Validation of species–climate impact models under climate change. Glob Change Biol 11:1504–1513

Bocheva L, Marinova T, Simeonov P, Gospodinov I (2009) Variability and trends of extreme precipitation events over Bulgaria (1961–2005). Atmos Res 93:490–497

Chen L, Frauenfeld OW (2014) A comprehensive evaluation of precipitation simulations over China based on CMIP5 multimodel ensemble projections. J Geophys Res Atmos 119:5767–5786

Ding Y, Sun Y, Wang Z, Zhu Y, Song Y (2009) Inter-decadal variation of the summer precipitation in China and its association with decreasing Asian summer monsoon Part II: possible causes. Int J Climatol 29:1926–1944

Dong Q, Chen X, Chen T (2011) Characteristics and changes of extreme precipitation in the Yellow-Huaihe and Yangtze-Huaihe rivers basins, China. J Clim 24:3781–3795

Easterling DR, Meehl GA, Parmesan C, Changnon SA, Karl TR, Mearns LO (2000) Climate extremes: observations, modeling, and impacts. Science 289:2068

Gong DY, Ho CH (2002) Shift in the summer rainfall over the Yangtze River valley in the late 1970s. Geophys Res Lett 29:1436

Gong DY, Ho CH (2003) Arctic oscillation signals in the East Asian summer monsoon. J Geophys Res 108:4066

Grimm AM (2011) Interannual climate variability in South America: impacts on seasonal precipitation, extreme events, and possible effects of climate change. Stoch Env Res Risk Assess 25:537–554

Groisman PY, Karl TR, Easterling DR, Knight RW, Jamason PF, Hennessy KJ, Suppiah R, Page CM, Wibig J, Fortuniak K (1999) Changes in the probability of heavy precipitation: important indicators of climatic change. Clim Change 42:243–283

Groisman PY, Knight RW, Easterling DR, Karl TR, Hegerl GC, Razuvaev VN (2005) Trends in intense precipitation in the climate record. J Clim 18:1326–1350

Huang NE, Wu Z (2008) A review on Hilbert-Huang transform: method and its applications to geophysical studies. Rev Geophys 46:1–23

Huang NE, Shen Z, Long SR, Wu MC, Shih HH, Zheng Q, Yen NC, Tung CC, Liu HH (1998) The empirical mode decomposition and the Hilbert spectrum for nonlinear and non-stationary time series analysis. Proc R Soc Lond A 454:903–995

Huang NE, Shen Z, Long SR (1999) A new view of nonlinear water waves: the Hilbert Spectrum 1. Annu Rev Fluid Mech 31:417–457

IPCC (2014) Climate change 2014: synthesis report. Contribution of Working Groups I, II and III to the Fifth Assessment Report of the Intergovernmental Panel on Climate Change

Iwashima T, Yamamoto R (1993) A statistical analysis of the extreme events: long-term trend of heavy daily precipitation. J Meteorol Soc Jpn 71:637–640

Jiang L, Mei W, Zhaohui L, Yu X, Xiaozong S, Xinhao G, Deshui T, Haitao L, Jianjun Z, Changsong L (2008) Situation analysis report of climatic change in Shandong Province. China Climate Change Partnership Framework, Beijing, pp 33–39

Jiang DJ, Li Z, Wang K (2011) Trends of extreme precipitation events over Shandong Province from 1961 to 2008. Sci Geogr Sin/Dili Kexue 31:1118–1125 **(in Chinese)**

Jiang F, Hu R, Wang S, Zhang Y, Tong L (2013) Trends of precipitation extremes during 1960–2008 in Xinjiang, the Northwest China. Theor Appl Climatol 111:133–148

Kalnay E, Kanamitsu M, Kistler R, Collins W, Deaven D, Gandin L, Iredell M, Saha S, White G, Woollen J (1996) The NCEP/NCAR 40-year reanalysis project. Bull Am Meteorol Soc 77:437–471

Karl TR, Knight RW, Easterling DR, Quayle RG (1996) Indices of climate change for the United States. Bull Am Meteorol Soc 77:279–292

Kendall MG (1970) Rank correlation methods. Griffin, London

Klein Tank A, Können GP (2003) Trends in indices of daily temperature and precipitation extremes in Europe, 1946–99. J Clim 16:3665–3680

Kunkel KE, Easterling DR, Redmond K, Hubbard K (2003) Temporal variations of extreme precipitation events in the United States: 1895–2000. Geophys Res Lett 30:1900

Lea DW, Pak DK, Spero HJ (2000) Climate impact of late Quaternary equatorial Pacific sea surface temperature variations. Science 289:1719–1724

Li Z, He Y, Wang P, Theakstone WH, An W, Wang X, Lu A, Zhang W, Cao W (2012) Changes of daily climate extremes in southwestern China during 1961–2008. Global Planet Change 80:255–272

Liu B, Xu M, Henderson M, Qi Y (2005) Observed trends of precipitation amount, frequency, and intensity in China, 1960–2000. J Geophys Res 110:D08103

Livezey RE, Chen WY (1983) Statistical field significance and its determination by Monte Carlo techniques. Mon Weather Rev 111:46–59

Mallakpour I, Villarini G (2015) The changing nature of flooding across the central United States. Nat Clim Change 5:250–254

Mann HB (1945) Nonparametric tests against trend. Econom J Econom Soc 13:245–259

Mearns LO, Katz RW, Schneider SH (1984) Extreme high-temperature events: changes in their probabilities with changes in mean temperature. J Clim Appl Meteorol 23:1601–1613

Meehl GA, Karl T, Easterling DR, Changnon SA, Pielke RA, Changnon D, Evans J, Groisman PY, Knutson TR, Kunkel KE (2000) An introduction to trends in extreme weather and climate events: observations, socioeconomic impacts, terrestrial ecological impacts, and model projections. Bull Am Meteorol Soc 81:413–416

Mishra AK, Singh VP (2010) Changes in extreme precipitation in Texas. J Geophys Res Atmos 1984–2012:115. doi:10.1029/2009JD013398

Moberg A, Jones PD, Lister D, Walther A, Brunet M, Jacobeit J, Alexander LV, Della-Marta PM, Luterbacher J, Yiou P (2006) Indices for daily temperature and precipitation extremes in Europe analyzed for the period 1901–2000. J Geophys Res 111:D22106

Nie C, Li H, Yang L, Ye B, Dai E, Wu S, Liu Y, Liao Y (2012) Spatial and temporal changes in extreme temperature and extreme precipitation in Guangxi. Quat Int 263:162–171

O'Gorman PA, Schneider T (2009) The physical basis for increases in precipitation extremes in simulations of 21st-century climate change. Proc Natl Acad Sci 106:14773–14777

Pachauri RK, Allen MR, Barros VR, Broome J, Cramer W, Christ R, Church JA, Clarke L, Dahe Q, Dasgupta P (2014) Climate change 2014: synthesis report. Contribution of Working Groups I, II and III to the Fifth Assessment Report of the Intergovernmental Panel on Climate Change

Peterson TC, Heim RR Jr, Hirsch R, Kaiser DP, Brooks H, Diffenbaugh NS, Dole RM, Giovannettone JP, Guirguis K, Karl TR (2013) Monitoring and understanding changes in heat waves, cold waves, floods, and droughts in the United States: state of knowledge. Bull Am Meteorol Soc 94:821–834

Powell EJ, Keim BD (2014) Trends in daily temperature and precipitation extremes for the southeastern United States: 1948–2012. J Clim 28:1592–1612

She D, Xia J (2013) The spatial and temporal analysis of dry spells in the Yellow River basin, China. Stoch Env Res Risk Assess 27:29–42

Sillmann J, Kharin VV, Zwiers FW, Zhang X, Bronaugh D (2013) Climate extremes indices in the CMIP5 multimodel ensemble: Part 2. Future climate projections. J Geophys Res Atmos 118:2473–2493

Tian Y, Xu YP, Booij MJ, Lin S, Zhang Q, Lou Z (2012) Detection of trends in precipitation extremes in Zhejiang, east China. Theor Appl Climatol 107:201–210

Villarini G, Smith JA, Vecchi GA (2013) Changing frequency of heavy rainfall over the central United States. J Clim 26:351–357

Wang H (2001) The weakening of the Asian monsoon circulation after the end of 1970's. Adv Atmos Sci 18:376–386

Wang L, Chen W (2014) A CMIP5 multimodel projection of future temperature, precipitation, and climatological drought in China. Int J Climatol 34:2059–2078

Wang Y, Zhou L (2005) Observed trends in extreme precipitation events in China during 1961–2001 and the associated changes in large-scale circulation. Geophys Res Lett 32:L09707

Wang B, Wu R, Lau KM (2001) Interannual variability of the Asian summer monsoon: contrasts between the Indian and the Western North Pacific-East Asian monsoons. J Clim 14:4073–4090

Wang W, Chen X, Shi P, Gelder PV (2008) Detecting changes in extreme precipitation and extreme streamflow in the Dongjiang River Basin in southern China. Hydrol Earth Syst Sci 12:207–221

Wang W, Shao Q, Yang T, Peng S, Yu Z, Taylor J, Xing W, Zhao C, Sun F (2013) Changes in daily temperature and precipitation extremes in the Yellow River Basin, China. Stoch Env Res Risk Assess 27:401–421

Wuebbles D, Meehl G, Hayhoe K, Karl TR, Kunkel K, Santer B, Wehner M, Colle B, Fischer EM, Fu R (2014) CMIP5 climate model analyses: climate extremes in the United States. Bull Am Meteorol Soc 95:571–583

Xie L, Pietrafesa LJ, Wu K (2002) Interannual and decadal variability of landfalling tropical cyclones in the southeast coastal states of the United States. Adv Atmos Sci 19:677–686

Yan G, Qi F, Wei L, Aigang L, Yu W, Jing Y, Aifang C, Yamin W, Yubo S, Li L (2014) Changes of daily climate extremes in Loess Plateau during 1960–2013. Quat Int 371:5–21

Yancheva G, Nowaczyk NR, Mingram J, Dulski P, Schettler G, Negendank JFW, Liu J, Sigman DM, Peterson LC, Haug GH (2007) Influence of the intertropical convergence zone on the East Asian monsoon. Nature 445:74–77

You Q, Kang S, Aguilar E, Pepin N, Flügel W, Yan Y, Xu Y, Zhang Y, Huang J (2011) Changes in daily climate extremes in China and their connection to the large scale atmospheric circulation during 1961–2003. Clim Dyn 36:2399–2417

Yue S, Pilon P (2004) A comparison of the power of the t test, Mann-Kendall and bootstrap tests for trend detection/Une comparaison de la puissance des tests t de Student, de Mann-Kendall et du bootstrap pour la détection de tendance. Hydrol Sci J 49:21–37

Zhai P, Sun A, Ren F, Liu X, Gao B, Zhang Q (1999) Changes of climate extremes in China. Clim Change 42:203–218

Zhai P, Zhang X, Wan H, Pan X (2005) Trends in total precipitation and frequency of daily precipitation extremes over China. J Clim 18:1096–1108

Zhang X, Yang F (2004) RClimDex (1.0) user manual. Climate Research Branch Environment Canada. http://etccdi.pacificclimate.org/RClimDex/RClimDexUserManual.doc

Zhang X, Hegerl G, Zwiers FW, Kenyon J (2005) Avoiding inhomogeneity in percentile-based indices of temperature extremes. J Clim 18:1641–1651

Zhang Q, Xu CY, Zhang Z, Chen YD, Liu C, Lin H (2008) Spatial and temporal variability of precipitation maxima during 1960–2005 in the Yangtze River basin and possible association with large-scale circulation. J Hydrol 353:215–227

Zhang X, Alexander L, Hegerl GC, Jones P, Tank AK, Peterson TC, Trewin B, Zwiers FW (2011) Indices for monitoring changes in extremes based on daily temperature and precipitation data. Wiley Interdiscip Rev Clim Change 2:851–870

Zhang Q, Xiao M, Singh VP, Chen X (2013) Copula-based risk evaluation of hydrological droughts in the East River basin, China. Stoch Env Res Risk Assess 27:1397–1406

Zhou B, Han Wen Q, Xu Y, Song L, Zhang X (2014) Projected changes in temperature and precipitation extremes in China by the CMIP5 multi-model ensembles. J Clim 27:6591–6611

Zhuo H, Zhao P, Zhou T (2014) Diurnal cycle of summer rainfall in Shandong of eastern China. Int J Climatol 34:742–750

Zou X, Zhai P, Zhang Q (2005) Variations in droughts over China: 1951–2003. Geophys Res Lett 32:L04707